Int. J. Electrochem. Sci., 14 **(2019)** 6347 – 6365, doi: 10.20964/2019.07.05

International Journal of ELECTROCHEMICAL SCIENCE
www.electrochemsci.org

Extraction of Epigallocatechin Gallate from Green Tea and its Chracterization using Polymeric electrode PAN/PPY enriched with nano particles of TiO_2 and rGO

Fatemeh Ferdosian, Mehdi Ebadi, Ramin Zafar-Mehrabian[*]*, Maziar Ahmadi Golsefidi and Ali Varasteh Moradi*

Department of Chemistry, Gorgan Branch, Islamic Azad University, Gorgan, Iran
[*]E-mail: raminzafar@yahoo.com

Received: 15 October 2018 / *Accepted:* 19 April 2018 / *Published:* 10 June 2019

Several publications have reported in the recent years documenting green tea and its flavonoid compounds, i.e. catechins. The article opens up a new issue on using electrochemical methods to identify, to measure and to increase the extraction efficiency of epigallocatechin gallate (EGCG). The conductive polymeric sorbent associated with nano materials was used to enhance the electrode's sensitivity. Conductive polymer electrodes were prepared using electrodeposition (EPD) and electrophoretic (EP). To illustrate the result, the structure of the polymeric electrodes (PAN/PPY/TiO_2/G) was investigated through FTIR analysis, FESEM-EDX, XRD, and electrochemical impedance spectroscopy (EIS). In order to identify and determine the concentration and purity of EGCG extracts, the following techniques were used: chronoamperometric technique with Potentiostat/Galvanostat instrument (AUTOLAB); (HPLC) and UV-Vis spectrophotometry. Our research has highlighted the importance of this method due to obtain high purity (76.02 ± 0.49). According to the results, it has been found that modified polymeric electrodes with nanoparticles (PAN/PPY/TiO_2/G) have high efficiency and low operating expense and less time-consuming to extract high purity EGCG.

Keywords: Electrochemically extraction; Conductive polymeric electrodes; Electrochemical synthesis; Epigallocatechin gallate (EGCG).

1. INTRODUCTION

Green tea (*Camellia sinensis*) is one of the medicinal plants, and is considered as one of the most traditional and the most popular drinks in the world [1]. Green tea has active chemical components called polyphenols (AmbePhytoextracts, GTPs) or flavonoids and has various medicinal properties comprising antioxidants, anti-inflammatory and antibacterial properties [2]. The most

important flavonoid in tea is flavonol or cathicine. Catechins are anti-oxidant and have anti-inflammatory, anti-microbial, anti-cancer and anti-mutagenic effects. Green catechins, for example, can prevent some skin and liver cancers and reduce lung and stomach cancer. Catechins are of particular importance in various industries such as pharmaceuticals, food, cosmetics and hygiene. For example, in pharmacy, producing toothpaste, mouthwash and breath freshener as well as complementary or drinking pills are used to increase the health of consumers. Catechins are found in foods like green tea, persimmons, apple and grapes [3,4].

Catechins were structurally divided into two groups: free catechins and esterified catechins. Free catechins include Catechin (C), Gallocatechin (GC), Epicatechin (EC), Epigallocatechin (EGC), while the esterified catechins are Epigallocatechin Gallate (EGCG), Epicatechin Gallate (ECG), Gallocatechin Gallate (GCG), and Catechin Gallate (CG). Esterified catechins have remarkable moisture content and have a bitter taste, while free catechins are very harmful and have a slightly sweet taste. The Catechins in tea are as follows: epigallocatechin (-) (EGC); Epicatechin (-) (EC); Catechin (C); Epicatechin gallate (-) (EGC), Gallocatechin Gallate (GCG) (-), Epigallocatechin Gallate (EGCG). The typical compound of green tea contains: epigallocatechin gallate (-) (EGCG) 10-15%, Epicatechin Gallate (-) (ECG) 6-10%, Epigallocatechin (-) (EGC) 2-3%, and epicatechin (-) (EC) 2% [5]. Among catechins, EGCG typically has the highest concentration, and EGC, ECG and EC are in the next levels. Researches have shown that the highest antioxidant properties of green tea are related to Epigallocatechin gallate [2-4].

Numeral researchers are considered for identification, determination, extraction and separation of these compounds. Identification and measurement of catechins have been greatly facilitated by chromatographic techniques, such as HPLC and CE, using various detectors such as UV, electrochemical, and MS detectors for the catechins analysis. Also, near-infrared spectroscopy, TLC and GC have been used for detecting and measuring catechins [6]. Currently, HPLC is the most common method for determining the Catechins of tea, because the separation is very good and can be combined with a set of detectors. The maximal UV-Vis absorption of catechins were found out at 210 and 269 to 280 nm [7].

The extraction efficiency of phenolic compounds and the antioxidant capacity of green tea depend greatly on extraction time and used solvent [8]. The most important items in extraction were introduced as solvent, distilled water [9], organic solvent [10], extraction using microwave [11], extraction by the subcritical water extraction supercritical fluid extraction (SWE-SFE) [12], ultrasound extraction (UAE) [13], extraction with solid phase [14], extraction by different filters [9], extraction by a variety of filters, extraction at ultra-high pressures extraction (UHPE) [15], extraction by molecular mold polymers and extraction by polymeric adsorbent [16].

Polymeric electrodes and conductive polymers have been used for the separation of bioactive compounds [17]. Polyaniline and polypyrrole were developed as the most commonly used Electro-copolymers. They have been used to fabricate the polymer electrodes due to their environmental stability, electrical properties, the adsorption of organic dyes from their solutions and their unique electrochemical properties between different conductive polymers [18]. Ateh his/her coworker. [19] have attempted to produce high-quality films for the separation of biological materials with the help of

electrochemical synthesis and the ability to control the thickness of matter and the possibility of doping during synthesis.

The refinement and optimization of the polymeric electrodes have been interested factor. The efficiency and durability of these materials were increased while Nanostructures in conjugated polymers were prepared [19]. Yang et al. [17] used the reinforced polymer electrode with nanostructures, to measure Epinephrine in the presence of uric acid and folic acid. Currently, graphene oxide, carbon nanoparticles, cellulose nanoparticles, Multiwall carbon nanotubes, and cadmium oxide nanoparticles have been used to modify polymeric electrodes [20].

To produce graphene-based materials, the graphene oxide was used in the structure of composites prepared by Anna his/her coworkers. [21] with this method that the efficiency of the prepared filters was increased through the using nanocomposites. In fact, in this type of nanocomposites, the main concern was on the relationship between the structural properties of the backbone materials in composite along with reinforcement of the nanocomposite properties.

Each of the aforementioned methods has some unmerites, such as unwanted residue from organic solvents in the final extracts in extraction with organic solvents, high temperature and high pressure in high pressure extraction (UHPE), and subcritical water extraction (SWE) and extraction with supercritical phase, unhealthy environmental effects through the use of microwave and ultrasound extraction, the low purity percentage of extraction in SPE methods, membrane filters and polymeric absorbent. Therefore, these methods were not consistent with the objectives of sustainable development (Green chemistry) and could not be used to increase industrial applied programs [22].

It is necessary to find methods that are not only simple, safe and inexpensive, but also having good accuracy, repeatability and high availability. Therefore, regarding their appropriate efficiency in term of high accuracy and precision, low cost and high speed of data collection, it seems that the electrochemical methods could be the good technique for fast and accurate analysis of the samples.

EGCG as a medicinal compound have been determined by many analytical techniques such as thin layer chromatography (TLC), high performance liquid chromatography (HPLC), Mass spectroscopy, and so on [22]. To the best of our knowledge, there were no reports to determine the mentioned compound using electrochemical methods. Therefore, this prompted us to determine the extracted EGCG by an electrochemical technique. It seems that the electrochemical methods are proper attempt due to the high accuracy, low cost, operation friendly and speed in the proper data collection. EGCG amount was qualified and quantified using differential pulse voltammetry (DPV) as a robust tool. That has been shown promising results in widespread electrochemical application such as evaluation performance of electrode/electrolytes. This technique based on physico-chemical phenomena. Calculating of impedance is carried out from Ohm's law: $Z= E/I$ where E is the electrical potential and I is the electrical current. Data presentation of EIS is governed by changes in current/ potential in counted frequencies to the determination of the electrochemical behavior of typical cell (electrodes), once a three-electrode compartment are used [23].

In the present study, the polymeric layers were enriched with nanomaterials to enhance the adsorption and efficient extraction. It could be controlled through the thickness of the material and doping on the surface of the electrode through electrochemical synthesis. High quality modified electrodes prepared by this method are used to dissolve the effective material of green tea. Therefore,

EGCG separation and purification are performed to increase the electrode's sensitivity using electrochemical methods and using conductive polymer nanocomposites.

2. MATERIAL AND METHODS

2.1 Materials and instruments

Aniline and Pyrrole were purchased from Sigma Aldrich Company. The distillations were done for three times to purification and separation of aniline and pyrrole from polymerized inhibitors in the vacuum condition and then, were kept in 5°C. Ammonium persulfate, hydrochloric acid 37%, propanol 99%, standard epigallocatechin gallate (EGCG, 99% purity), Sodium dodecylbenzenesulfonate (99% purity) were purchased from Fluka company (Germany). Graphene and titanium oxide (3-5 layers) was purchased from Merck (Germany). All solvents such as ethanol, methanol, and acetone were purchased from the Merck Company (Germany).

2.2 In situ polymerization and Fabrication of PAN/PPY/TiO2/G nanocomposite

At first, a mixture of graphene and titanium oxide nanoparticles was prepared. Graphene nanoparticles were dispersed at 5% W/W of polyaniline/polypyrrole copolymer in pure ethanol solution and were dispersed in the ultrasonic bath for 2 hours. Titanium dioxide nanoparticles were added to 3% W/W dispersed the mixture of polyaniline/polypyrrole copolymer.

The mixture was homogenized with ultrasonic waves for 30 minutes. Subsequently, polyaniline/polypyrrole/titanium dioxide/graphene was synthesized through *in situ* method. The homogenized nanoparticle mixture was added to 50 ml of the solution containing 155 mM aniline monomer and 155 mM freshly distilled pyrrole was added to an aqueous solution of 1.5 M HCl. Then, it was stirred for 1 h. The pH of the solution was adjusted to 4 over the entire synthesis period. The reaction mixture was placed in an ice bath at 5℃. 50 mL solution containing 310 mM ammonium persulfate (as oxidant) was added to the mixture containing monomer as drops for 1 h. The change in the color of the reaction mixture indicates the beginning of the polymerization. After adding all the oxidants, the reaction was processed for 24 h with continuous stirring to complete the polymerization. The reaction mixture was filtered with ethanol and acetone and then, was completely washed with distilled water. The obtained precipitation was again washed with distilled water, and the solid material was dried at 61 ℃ for 24 h in an oven [24].

2.3 Fabrication of PAN/PPY/TiO2/G Polymeric Electrodes by Electrophoretic method (E_I)

Electrophoretic-coating of synthesized particles as a thin film on the Fluorine-doped tin oxide (FTO) glasses were performed as follows: nanoparticles were dispersed (1h) in propanol 70% using the ultrasonic bath. FTO surface (1×1 cm^2) was degreased in acetone an ethanol solvent, respectively. The surface of FTO electrochemically coated by nanocomposite particles (Ppy/Pan/TiO_2/GO) when it was connected to the cathode clips and the anode was Platinum (equal surface size) and those were

immersed in propanol 70% containing mentioned particles. The electrical potential was applied with a DC digital supply. Variables items were: time (5, 10, 15 and 20 min), applied voltages (40, 50, 70 and 80 V), particles amount in the solution (0.1, 0.01 and 0.001 gr in 100 ml) and distance between anode and cathode (2.5, 5, 7 and 9 cm) (Fig.1).

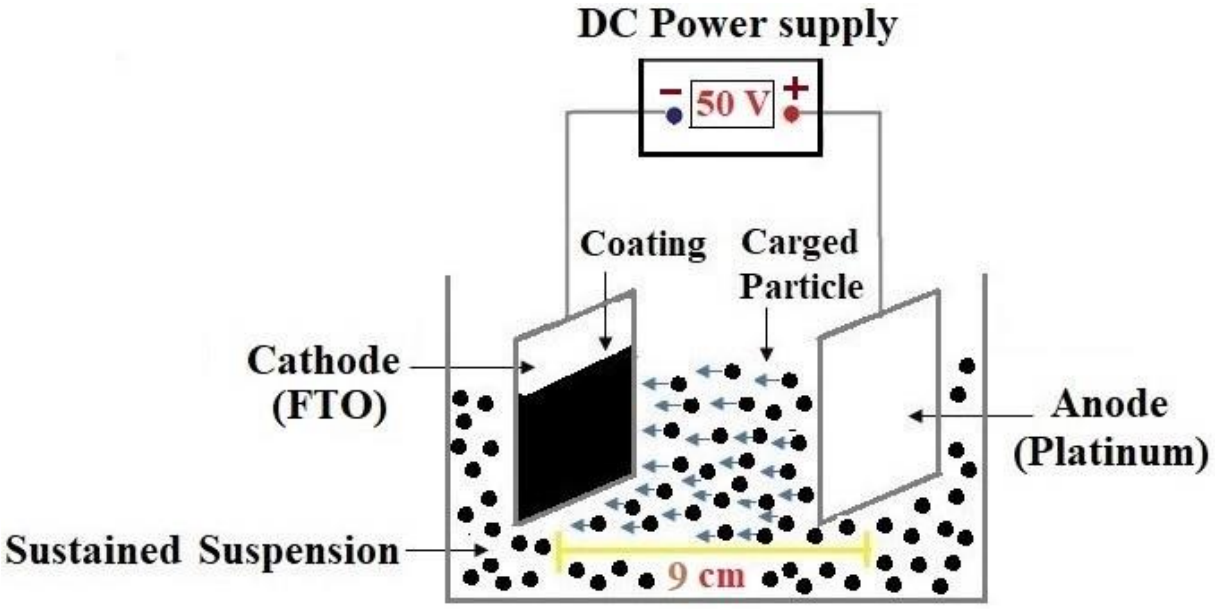

Figure 1. Schematic of the Electrophoretic coating process.

2.4 Fabrication of PAN/PPY/TiO2/G Polymeric Electrodes by Electrodeposition method (E_{II})

Graphene oxide and titanium dioxide nanoparticles were weighted 5%W/W compared to polyaniline/polypyrrole copolymer. The mixture of nanoparticles was dispersed in ethanol in the ultrasonic bath for 2 hours. The mixture of completely homogenized nanoparticles was added to a solution containing aniline monomer (155 mM) and freshly dispersed pyrrole (155 mM) in the aqueous solution of HCl 1.5 M. The solution pH was set to 4 over the entire synthesis process a cyclic voltammetric technique was used for electrodeposition operation. The potential range was set to -0.4 and 1.3 V (*vs.* Ag / AgCl electrode) at scan rate 20 mV sec^{-1}. The electrode was fabricated by 50 cycles.

2.5 Characterization of electrodes

The following techniques were used to evaluate the quality of the layers fabricated on the FTO surface. Fourier transform infrared ray spectroscopy (FTIR) was performed in the range of 1400-4000 cm^{-1}. X-ray diffraction (XRD: PHILIPS XPERT instrument) was used to study the crystalline structure of coated nanocomposites. X-ray diffraction patterns were prepared with Cukθ radiation in the range of 2θ = 0-80 ° for 40 kV and 40 mA, and the scan rate was 20 mV min^{-1}. The scanning electron

microscopy equipped with elemental analysis (FESEM-EDX-MIRA3) was used to study the nanoparticle diffusion in the produced nano-composite system.

2.5.1 EIS studies of both electrodes (E_I) & (E_{II})

Electrochemical Impedance Spectroscopy (EIS) measurements for both (E_I) and (E_{II}) were studied through the Nyquist plot in 0.5 M Na_2SO_4. The EIS measurements were performed at the open circuit potential, with a Vrms of 10 mV and a frequency range between 100 kHz–10 MHz, using the frequency response analyzer (FRA) software installed in a computer and interfaced with Autolab 240. Not only the three-electrode configuration as Pt wire (equal area with the WE: FTO coated) were used as the counter electrode at a fixed potential of 0 V *vs.* Ag/AgCl but also it was set for all electrochemical process in this study.

2.5.2 Adsorption and desorption of EGCG from Standard Solution through the Physical and Chronoamperometry Method

Physical method: polymeric electrode of PAN/PPY/TiO2/G produced by electrophoretic method was transferred to 30 ml of EGCG solution 10 ppm (aqueous solution). The adsorption of EGCG was carried out at room temperature (RM) for 2 h and pH=4. Moreover, desorption of this electrode was carried out in 30 ml of distilled water at RM and at pH = 4 during 1 h.

Electrochemical method: To measure the adsorption and desorption of the EGCG from the standard solution through an electrochemical method (chronoamperometry), the AUTOLAB instrument, Gstat 302N/Pstat model was used as a source of potential or current that is connected to the computer equipped with GPES. Polymeric electrodes of PAN/PPY/TiO2/G produced by electrophoretic and electrodeposition methods in 30 ml of EGCG 10 ppm (aqueous solution) under RT condition and pH = 4 in the AUTOLAB instruments. The adsorption process was 1200 sec at -1.3 V and the desorption time of EGCG was 600 sec at +1 V in three repetitions [25].

2.5.3 Measurement of adsorption/desorption of EGCG using HPLC technique

Column chromatography with high yield was used to determine the concentration of physical and electrochemical adsorption and desorption. 20 µl control solution and the remained solution from the adsorption and desorption process was injected into the instrument (HPLC Agilent ZOR BOX XDB-C18). In both measurements, the UV detector was set at 280 nm. The column was C18 in 15 cm length. Acetonitrile 8% and phosphoric acid 95% were used as a mobile phase with gradient flow [22].

2.5.4 Electrochemically extraction of EGCG and determination with HPLC and UV-Vis methods

In this study, a steeping method was used to extract green tea [22]. Subsequently, chromatography column (silica gel 60) was used to separate and purify the catechins contained in the

extract with organic solvents (n-hexane, and ethyl acetate and N- butane) [26]. The initial identification of EGCG in each extraction volume was performed from the chromatography column (by mobile phase: n-hexane: ethyl acetate with a ratio of 75:25) through the TLC technique [22]. In order to qualitative and quantitative evaluation of EGCG, HPLC was used for each of the components obtained from chromatography column [22]. 20 µl standard EgCg solution (10 ppm) as control and 20 µl each of the obtained fractions was injected into HPLC instrument including UV detector at 280 nm and column C18 in 15 cm length. After identification and measurement, the sample was selected from the sample containing the highest amount of epigallocatechin gallate. This sample was kept at 3 °C in dark. This sample was used to test electrochemical adsorption and desorption tests using electrodes prepared by electrophoretic and electrodeposition methods.

To confirm the HPLC results, the calibration curve was used from different concentrations. First, 100 ppm solution was prepared as a stock solution. Then, the working solutions were prepared: 0.25 ppm, 1 ppm, 2.5 ppm, 5 ppm, 10 ppm, 15 ppm, 25 ppm and the 50 ppm. Different concentrations were used to plot the calibration curve. 10 ml of EGCG standard solution (10 ppm) as control and 10 ml of adsorption solutions and 10 ml of solution from desorption solution obtained by chronoamperometry technique was placed at spectrophotometer as a sample. The amount of analyte adsorption was recorded by the spectrophotometer at 280 nm [22].

3. RESULTS AND DISCUSSION

3.1 The fabrication of the modified polymeric electrodes (PAN/PPY/TiO_2/G) Electrode (E_I) through the electrophoretic method (EPD)

Visually, it was found that the electrodes with PAN/PPY/TiO_2/G nanocomposite had the best deposition on the FTO with following conditions: the concentration of 0.01 $g.l^{-1}$ while the distance of two electrodes was 9 cm, applied potential was maximal at 50 V for 20 min. The FTO glass was weighed before and after the electrophoretic method. The amount of deposited nanocomposite on the FTO glass electrode was 0.001 g/cm^2. The conductivity of the prepared electrodes by the voltmeter was measured. The resistivity of two electrodes (distance: 1 cm) was determined by voltammeter and it was found that diminished to zero during 3 sec. furthermore, the applied voltage was optimal (50 V) to deposit the layer, so that the nanocomposite structure is entirely intact during electrophoretic operations. It will be explained in FTIR, XRD and FESEM-EDX studies sections. Du and his research group [27] have successfully made an ultrasensitive electrode using electrophoretic technique.

3.2 Fabrication of electrode (E_{II}) through the electrodeposition (EP):

Electrochemically, nanocomposites PAN/PPY, PAN/PPY/TiO_2 and PAN/PPY/TiO2/G were polymerized on the FTO using the cyclic voltammetric technique (50 cycles) at the potential range between -0.4 and +1.3, the scan rate 20 mV s^{-1} (*vs.* Ag/AgCl). The observed peak at 0.81 V was assisted to the PAN/PPY copolymer (Fig. 2a). The effect of increasing titanium oxide and graphene

nanoparticles in the PAN/PPY chemical shift is quite evident, as the mentioned peak was shifted at 1.38 V and 0.89 V by increasing TiO_2 and G, respectively (Fig.2b). the conductivity of the film was decreased as TiO_2 increases, and in contrast, the conductivity of the film is increased by increasing G (Fig. 2c). The obtained results were compromised with other researchers' results, as they have shown that the conductivity of polymers was enhanced once the graphene nanolayers were embedded in the conductive polymers [23-28].

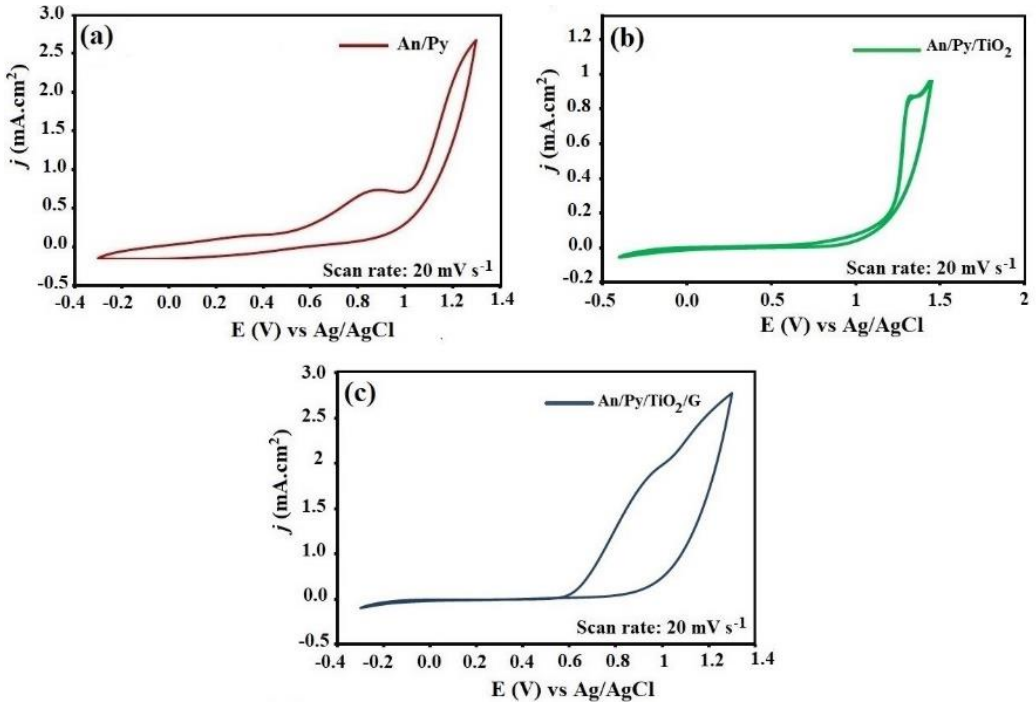

Figure 2. Cyclic voltammograms of the electrodes during the synthesis process for (a): An/Py (b): An/Py/TiO_2 (C): An/ Pn/TiO_2/G through the (EP).

3.3 FTIR studies of (E_I) and (E_{II}) electrodes:

The PAN/PPY/TiO2/G prepared nanocomposites were analyzed by infrared spectroscopy (FTIR). Characteristic peaks are as follows (Fig. 3). The observed peak was around 1400 cm^{-1} area related to bonding vibration in Ti-O-Ti at the TiO_2 structure. The observed peak in the 3400 cm^{-1} refers to the vibrational stretching of O-H bond that is due to the adsorbed water on the surface by nanocomposites [29]. The appeared peaks of graphene/graphene oxide was reported in 1200 cm^{-1} and 1580 cm^{-1} which are assisted to vibrational stretching of C-O and aromatic C=C [30].

The relatively high peak intensity in 1400 cm^{-1} and 1600 cm^{-1} is due to the strong interaction between the surface of the graphene plates and TiO2 nanoparticles. In graphene bonding with TiO_2, this interaction can form Ti-O-C vibrational bond in a lower field of 1630 cm^{-1} [30]. The obtained peak of C=C in 1530 cm^{-1} and 1460 cm^{-1} corresponds to the vibrational stretching in the quadrilateral ring in PANI (quinidine) and vibrational stretching of C=C in the benzene ring units, respectively.

The slight shifting in the observed wave numbers for the mentioned peaks can be attributed to π-π interactions and hydrogen bonding between graphene plates [30]. Also, the peak related to vibrations of the graphite main chain (carbon skeleton) has been reported in the 1637 cm^{-1}. The observed short peak in 1160 cm^{-1} was related to the flexural vibration on the C-H bond in the PANI [31]. The appeared peak in about 1400 cm^{-1} and 2000 cm^{-1} attributed to the vibrational stretching of the C-N bond in the Pyrrole ring and the formation of PPY in the final structure [32]. The resulting FTIR peaks represent the presence of all expected components and the proper interaction between the functional groups of the nanocomposite components. This result suggests that this method is an appropriate method for the preparation of nanocomposites.

The polymeric layer spectrum peeled off from the electrode surface prepared by EPD and EP methods have completed overlapping with the synthesized nanocomposite spectrum (Fig. 3a-c). This point confirms the presence of all nanocomposite components at the electrodes surface (E_I) and (E_{II}). It also shows that the voltage and used techniques are appropriate because the structure of the nanocomposite has been fully protected during the synthesis of electrodes.

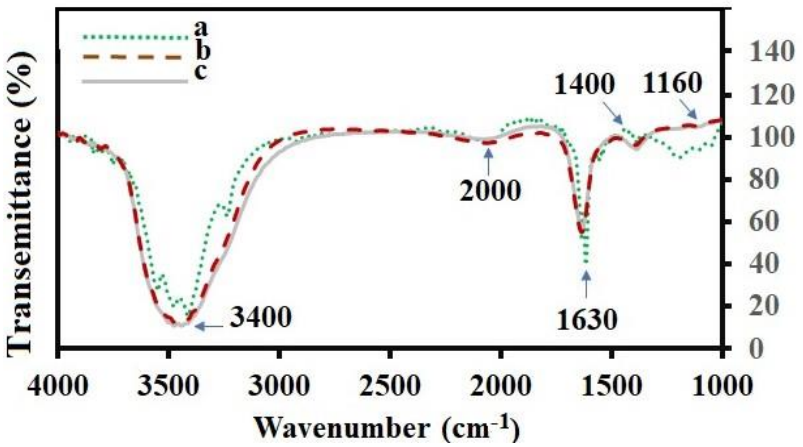

Figure 3. The complete overlap of FTIR spectra of (a). Nanocomposite PAN/PPY/TiO2/G (b), Electrode (E_I) and (c) Electrode (E_{II}).

3.4 XRD characterization:

The x-ray diffraction of polymeric electrodes (E_I) and (E_{II}) was shown in Fig. (4a, b). In the Fig. (4a) peaks show the presence of TiO_2 in the anatase phase at 75, 68, 62, 55, 54, 48 and 38, and 2θ=25°, with (101), (103), (200), (004), (213), (104) and (215) the plates (JCPDS No: 88-1175 and 84-1286). Peaks with (004) and (104) and (112) planes at angles 2θ= 53, 63 and 70° were related to carbon content in the graphene network (JCPDS NO; 01-075-1621) The presence of a broad peak in the 2θ=25 indicates the presence of polyaniline (Card No. 81-2261) and Polypyrrole in the nanocomposite, simultaneously [33].

Regarding the XRD related to pure polypyrrole and polyaniline, shifting the broad peak of pure polypyrrole and polyaniline in the 2θ=25 could be due to the formation of polypyrrole and polyaniline copolymer and an appropriate interaction between the titanium oxide nanoparticle with graphene and

the components of polypyrrole and polyaniline copolymer. The same condition as shown in the electrode (E_{II}) can be seen in Fig. (4b).

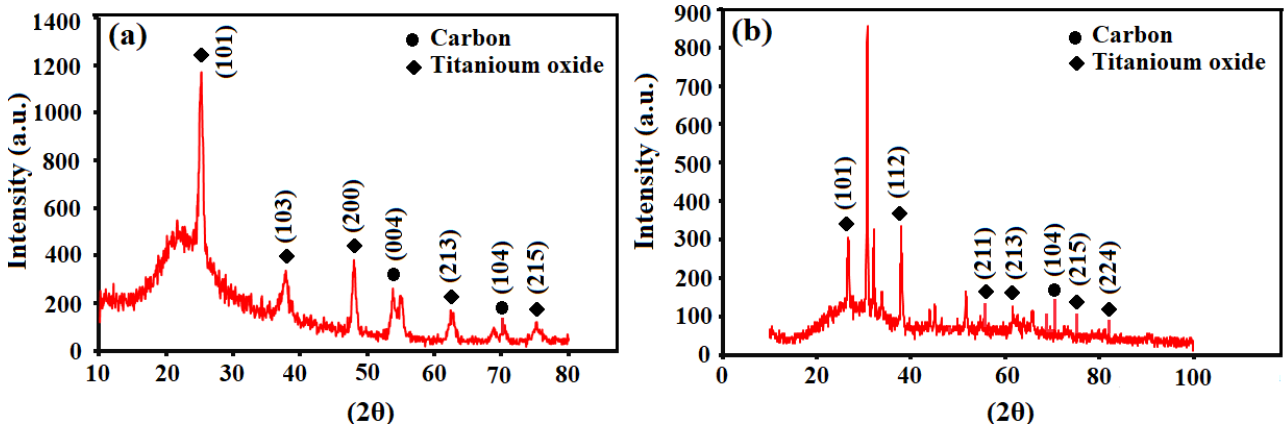

Figure 4. XRD spectrum of a): electrophoretically deposited layers and b): Electrodeposited films.

3.5 FESEM/EDX studies

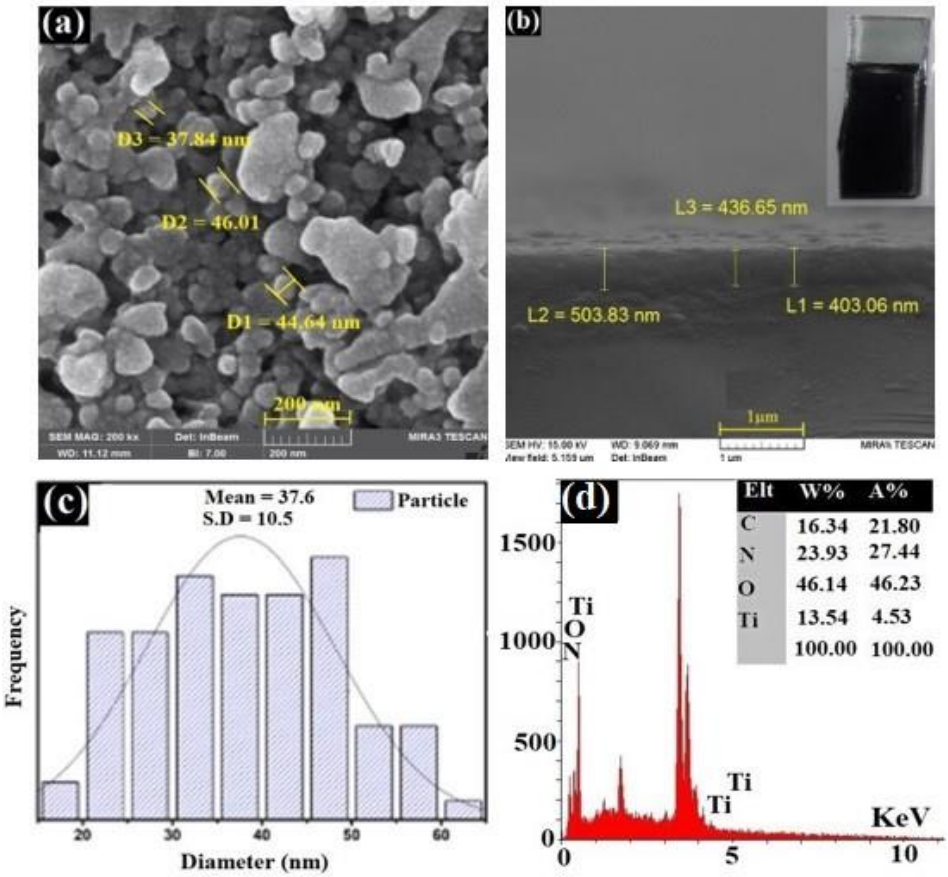

Figure 5. (a) FESEM/EDX of synthesized polymeric electrode (EI) by EPD method (b) Cross-sectional SEM false-colored image of Ppy/Pan/TiO_2/rGO sample composite on FTO substrate prepared by electrophoretic deposition (*inset electrode photograph*), (c) corresponding histogram of capsulated particles size distribution in (a) Gaussian fit curve is shown in black, (d) EDX spectrum of sample composite with corresponding atomic and weight percentage of C, N, O and Ti.

FESEM images equipped with EDX was used to identify the structure and elemental analysis of modified polymeric electrodes (E_I) and (E_{II}) (Fig. 5a-d) and (6a, d). The obtained FESEM images for polypyrrole and polyaniline copolymer show that it has a porous structure. Moreover, there is a tendency to accumulate and to form larger clusters and strings among the synthesized copolymer components. The interaction between polymer strings leads to the formation of such a structure.

The layered structure was related to graphene nanoparticles. The graphene has surrounded copolymer components and titanium oxide nanoparticles as a layer and has created continuous structure. The thickness of deposited layers was determined using FESEM through the cross section as E_I= 445 nm and E_{II}=725 nm, respectively. It has to be mentioned that both masses of deposited layers was the same, however; the electrodeposited layer for E_{II} was more compacted compared to E_I. In addition to the complete continuous, homogeneous dispersion of the copolymer components and graphene and titanium oxide nanoparticles was evident in the image. In many articles, graphene has been used as an adsorbent [34]. Therefore, the presence of graphene helps to optimally adsorption of EGCG.

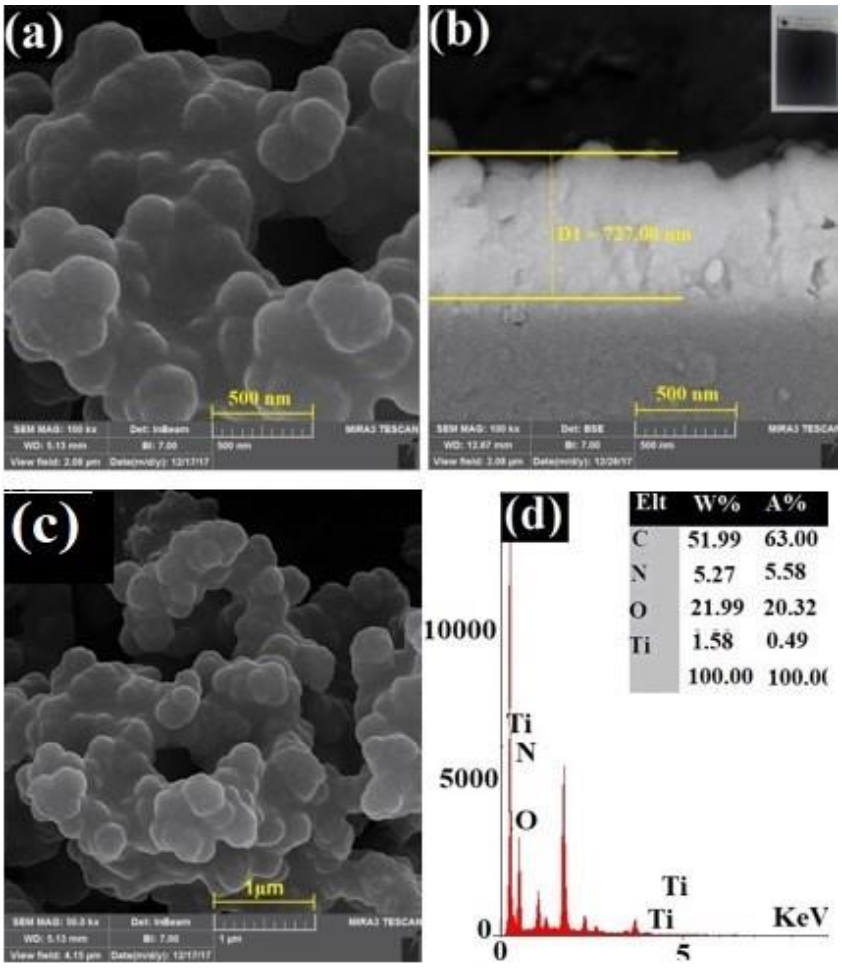

Figure 6. (a,d) FESEM/EDX of synthesized polymeric electrode (E_{II}) by EP method (b) Cross-sectional SEM false-colored image of Ppy/Pan/TiO_2/rGO sample composite on FTO substrate prepared by electrodeposition (*inset electrode photograph*), (d) EDX spectrum of sample composite with corresponding atomic and weight percentage of C, N, O and Ti.

3.6 Preparation of green tea extract and extraction of catechins

The extract was done from 5 g dried green tea leaves by a dilution method [22] that was transferred to the chromatography column. The carried out fractions were testified by the HPLC method. According to the results of HPLC, the fraction containing the highest amount of EGCG (0.50 ppm) and the lowest amount of interface was selected for extraction by electrochemical method (it will be displayed in Fig. 8b & b').

3.7 Electrochemical impedance measurements

Porous electrodes have been shown many merits for electrochemical approaches such as capacitance and adsorption. The most advantage of electrodes was carried out due to the large surface area of them. The adsorbed amount of species on the electrodes surface are depended on both conductivity, surface area of electrodes and applied voltage, as well. The conductivity of electrochemical electrodes could be studied by Electrochemical Impedance spectroscopy (EIS), while the associated equivalent circuits of electrodes was released from excellent fitting of EIS data, as shown in Fig. 7.

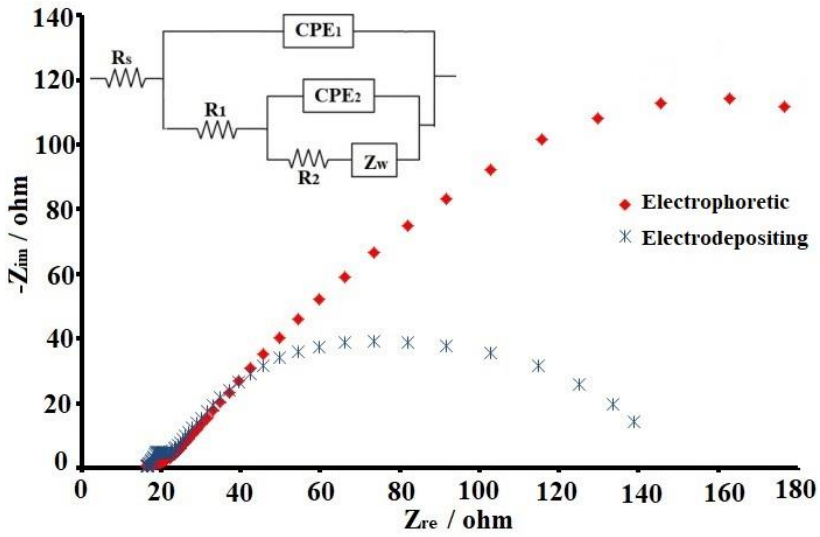

Figure 7. The obtained electrochemical impedance spectra (EIS) in both electrodeposited and electrophoretic conditions at bias-free potential *vs* Ag/AgCl using 0.1 M KCl solution.

Table 1. The obtained corresponding parameters using the simulation technique through the equivalent circuit analogs modeling for electrodeposited and electrophoretic deposited samples.

	R_s (Ω)	R_1 (Ω)	Q_1 (Y_o) (mMho)	n	Q_2 (Y_o) (mMho)	n	R_2 (Ω)	W (mMho)	S/cm
Elcttrophorethic	15.75	8.32	450.2	0.57	673.24	0.63	888.9	15.86	1.124
Electrodeposition	16.10	11.96	859.52	0.78	642.64	0.81	127.3	23.04	7.812

Two typical electrodes were evaluated by electrochemical impedance technique (Nyquist plot) in the same condition using equal-concentration of KCl. It was shown that the small arc radius was achieved for the synthesized electrodepositing electrode (Fig. 7) while the larger arc was obtained for electrophoretic (E_I) obtained electrode in the mentioned condition, as well. To study the more detail of electrochemical behavior of fabricated layers, due to the excellent fitting the equivalent circuit **[**R_s-(Q1 **|** (R1-(Q2 **|** R2-W))**]** with to relaxation time were resulted by the chi-square 10^{-6}. The first (Q1R1) and second (Q2R2-W) loops of the equivalent circuit were noticed the fabricated layer and conducting surface layer of FTO, respectively. Where R_s is the solution resistance, R1 and R2 are the resistance of the deposited layer and conducting layer of FTO to the electron transfer. Constance phase element (CPE) was instead of Q element to show the electrical double layer capacitance behavior for both electrodes. Moreover, the Warburg (W) element appeared due to diffusion of ion Cl^- to the fabricated layer. Excellent agreement between experimental and simulation data was achieved through the best fitting, that it was led to the electrical analogs parameters which tabulated in Table 1. The calculated conductivity of electrodeposited and electrophoretic deposited electrodes was 7.812 S/cm and 1.124 S/cm, respectively. Noteworthy, the calculated conductivities were proportional to electro-resistivity (arc of curves at Nyguist plot in Fig. 7). The charge transfer of electrodes have been investigated by scientists and it has been found that the curves with the great diameter of arc led to low conductivity compared to the curves with a small arc diameter [23-28].

3.8 Determination of EgCg Using NDPV method

The current−potential (i−E) curves were recorded using the polarographic analyzer. A rotating disc electrode (0.3 cm^2) with 1000 rpm as a working electrode, an Ag/AgCl as a reference and a Pt-foil as auxiliary electrode were used. A solution of EgCg (pH= 4) was adjusted with acetic acid 0.1 M. The concentration of EgCg in the analyzing solutions was obtained by standard addition method through the Normal Differential Pulse Voltammetry (NDPV) mode while 50 µl of understudying solutions (rest and extracted from 10 ppm solutions) was diluted (400 times) in electrolyte of electrochemical cell. In addition, electrolytes were buffered in above-mentioned pH. Before each i−E curve recording, the solution of the cell was purged by the stream of pure nitrogen, for 5 min before the first recording and during 30 s after the addition of each aliquot. The analyzed potentials were 0.6 to -0.15 V, while the potential scan rate was 10 mV s^{-1}, pulse amplitude 0.05 V, pulse time 0.04 s and voltage step 6 mV. All experiments were done in triplicate, at room temperature.

Electroactivity of EgCg 10 ppm was typically quantified and qualified using DC voltammetry technique. NDPV method- which has been known for a trace amount of electroactive analyte- was used to determine EgCg content in pH=4 solution at room temperature. To determine oxidizing the potential of EgCg, 50 µl of 10 ppm of the aqueous standard solution was added to 20 ml voltammography cell in each calibrating steps. The measurement was conducted in a three-electrode configuration rotating disc electrode (WE), platinum plate as a (CE) and Ag/AgCl reference electrode. The potential was scanned in the range of +0.6 to -1.5 V. The catechines oxidation behavior was studied by Janeiro's research group [25] and it was found that the valuable pH for oxidation of

catechines was around the natural range. However, the oxidation process of catechines will be disturbed while the pH is out of the mentioned range.

As demonstrated in Fig. 8, two characteristic peaks appeared at 0.0 and -1.0 V (vs. Ag/AgCl). By increasing the appropriate amount of standard solution in the sample, the intensity of these peaks started to enhance, confirming the presence of EgCg in the environment comes from increasing the analyte concentration. The concentration of trace EgCg in the sample was calculated by extrapolating the linear fit of the calibration curve (inset in Fig. 8) to be 9.24 ppm. To the best of the authors' knowledge, the reduction of EgCg was not reported. However, the oxidation of EgCg was examined by numerous scientists such as Masoum his/her coworkers. [35] with square wave voltammetry and Differential pulse voltammograms, respectively. Results obtained from DC voltammetry confirm successful extraction method in this study.

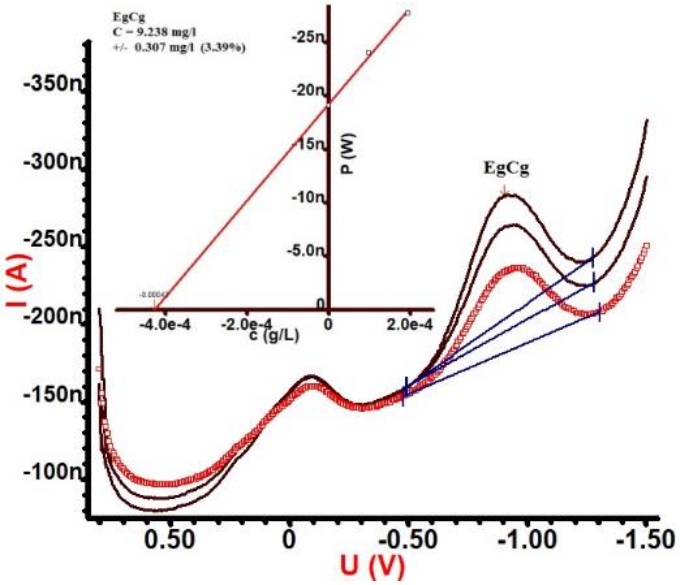

Figure 8. Voltammogram of EgCg (Inset calibration curve with a linear fit)

3.9 Electrochemically adsorption/desorption of EGCG

Measurement of adsorption and desorption rate of EGCG by electrochemical method (chronoamperometry) was performed by EPD and EP methods with synthesized polymeric electrodes PAN/PPY/TiO2/G. Adsorption and desorption of EGCG were carried out during 3600 sec at -1.3 V and 1800 sec at +1 V, respectively (three replications). The graphs of the EGCG absorption and desorption by the electrode (E_I) and (E_{II}) from the standard solution and the actual sample represented in Fig. 9 Ebadi and his research group. [23] have also used the chronoamperometry technique to desorption of Ni-Co-Fe-Zn in the dimethyl sulfoxide (DMSO) in the presence of magnetic field.

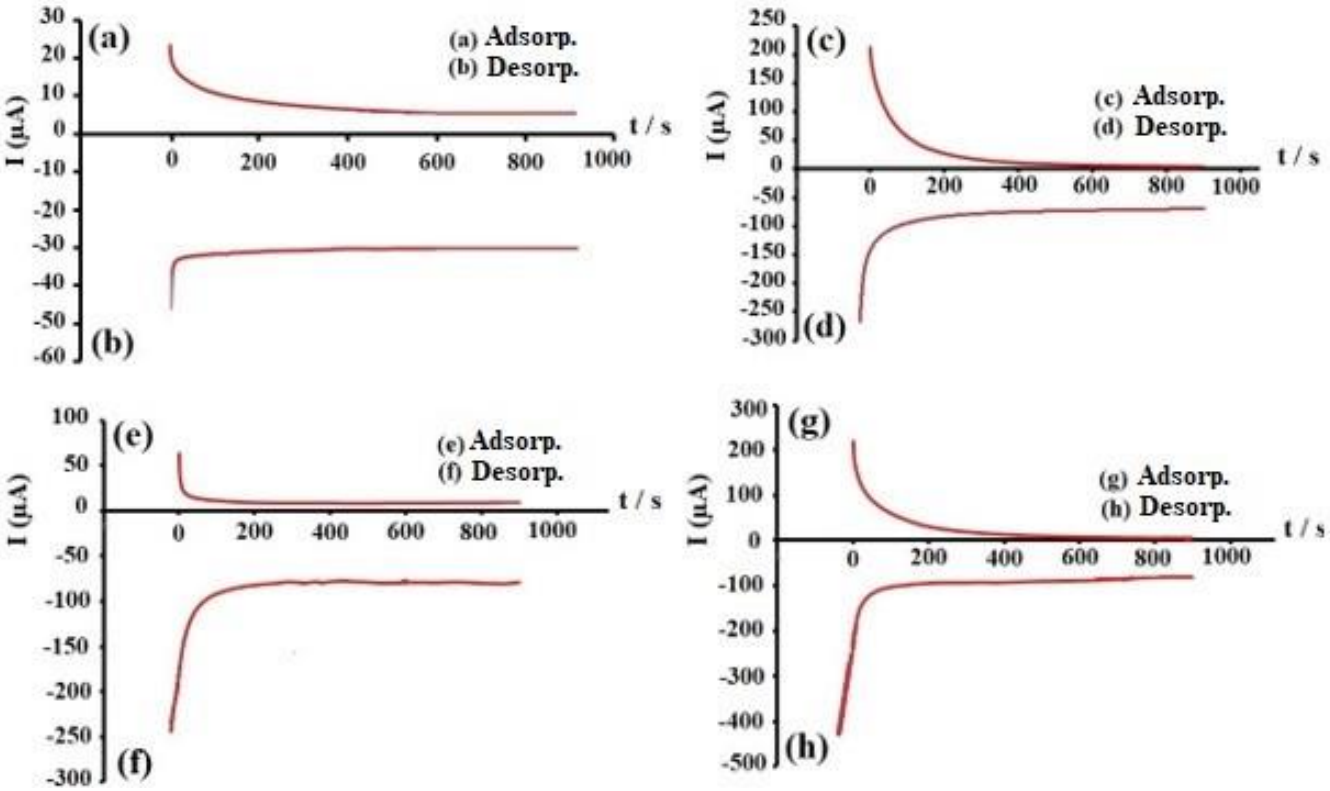

Figure 9. The curves of "a and b" and "c and d" are respectively the EGCG adsorption and desorption curve by the electrode (E_I) and (E_{II}) from the standard solution and the curves "e, and f" and "g and h" show the EGCG adsorption and desorption curve by Electrode (E_I) and (E_{II}) from an actual sample, respectively.

3.10 Measuring the extracted EGCG from standard solution (SS) and actual sample by HPLC and UV-vis technique

Polymeric electrodes (E_I) and (E_{II}) were used to extract EGCG from standard solution and actual sample. As an example, HPLC spectra of standard solution and actual samples, as well as the rest of electrolyte HPLC spectra from adsorption and desorption of electrode (E_{II}) has been shown in Fig. (10a-d). Figure (10a) illustrates the standard calibration curve for EGCG. In HPLC spectra of standard solutions with different concentrations, strong peaks appear at retention time around 9 min and at 280 nm wavelengths with UV detectors. It can be observed that with increasing concentration of the analyte, the adsorption increases at 280 nm wavelength. Figure (10b) shows HPLC spectrum related to the extract of green tea. The peak at retention time of 9 min was related to EGCG. Figure (10b') shows the HPLC spectrum corresponds to the actual sample obtained from the chromatographic column. The HPLC spectra of the rest of the solution from adsorption and desorption are presented in Figs. 9c and 9d. Comparison of these two spectra with the HPLC spectrum of the actual sample (Fig. 10b) showed the highest amount of EGCG. In the obtained spectra, the lowest peak impurities associated with impurities (peak NO. 1) in comparison to the standard solution.

The obtained data from the peak area (HPLC) were presented in Table 2. Consequently, it was observed that the physically extraction efficiency of EGCG was 7.23 ± 0.17% and 10.98 ± 0.41%

using E_I and E_{II}, respectively (SS). However, the electrochemically extraction efficiency of the mentioned analyte using E_I and E_{II} was 13.81 ± 0.79% and 61.70 ± 0.46%, respectively (from SS).

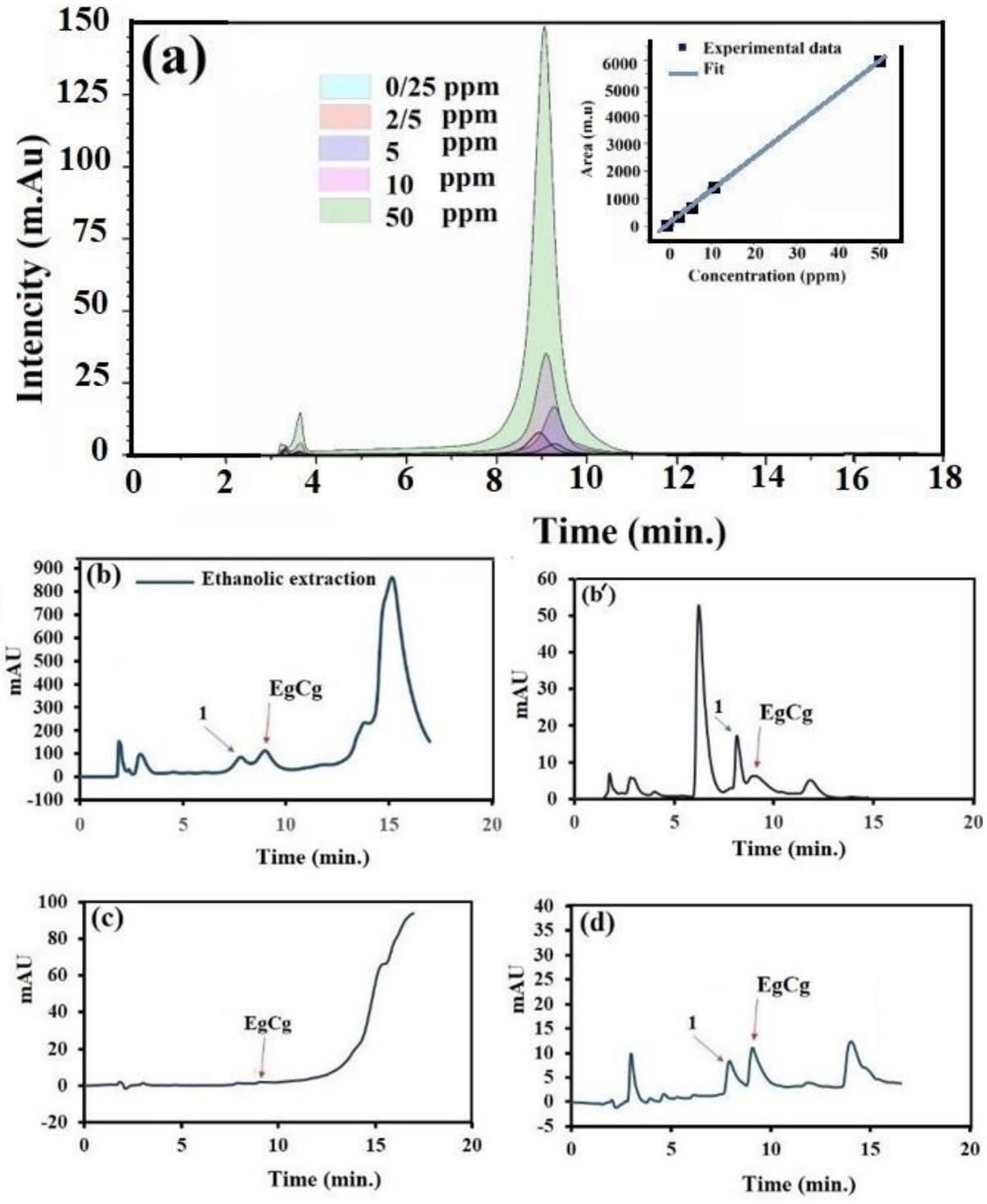

Figure 10. calibration curve of (a) Standard solution EgCg. (b) A green tea ethanolic extraction (b') The solution of EgCg obtained from the chromatography column (c,d) Adsorption and desorption EgCg by the electrochemical method from the actual sample with the electrode (E_{II}).

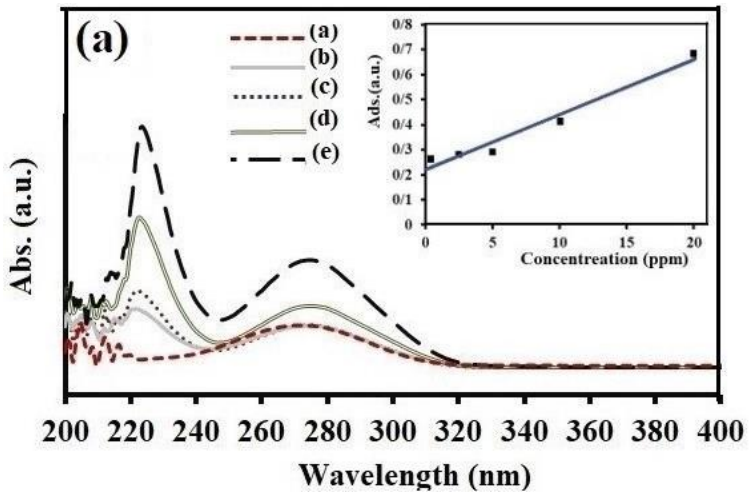

Figure 11. (a). The UV-VIS spectroscopy calibration curve with the EGCG standard solution at (a) 0.25ppm, (b) 2.5ppm, (c) 5ppm, (d) 10ppm, and 20ppm (e).

Regarding to the obtained results, it was found that both manufactured electrodes were useful for extraction of EgCg. Whatever, the electrochemically extraction was significantly efficient compared to physically extraction. Therefore, the extraction of EgCg from the natural samples was electrochemically performed using both of them. The results of quantitative and qualitative measurements through the HPLC technique showed that the EGCG extraction efficiency from the actual sample is 76.02 ± 0.49% > 3.4 ±0.05% by electrodes E_{II} and E_I, respectively. These results were also confirmed by UV-Vis spectroscopy.

Table 2. HPLC chromatographic information on adsorption and desorption of EGCG from standard solution and natural sample

Sample	Adsorp (ppm)		Desorp.. (ppm)		Area (ppm)		Extraction Efficiency %
	Phys.	Electroch.	Phys.	Electroch.	Adsorp.	Desorp.	
St. Sol. EgCg (10 ppm)	-	-	-	-	2526.23		-
E_I	0.79	-	0.72	-	204.22	186.125	7.23 ± 0.17
E_I	-	2.038	-	1.38	526.888	356.84	13.81 ± 0.79
E_{II}	5.3	-	1.098	-	1338.427	511.96	10.98 ± 0.41
E_{iI}	-	7.7	-	6.17	1990.64	1595.222	61.70 ± 0.46
S*	-	-	-	-	7867.758		-
S**	-	-	-	-	245.091		-
E_I	-	0.19	-	0.017	152.17	8.38	3.40 ± 0.05
E_{II}	-	0.45	-	0.38	21.84	188.35	76.02 ± 0.49

Note: S*: EgCg extracted from green tea (1.1 ppm/g).

S:** The Solution of the EgCg obtained from the chromatography column (0.5 ppm).

The calibration curve of EGCG standard solution was shown in Figure 11a. In UV-Vis spectra, standard solutions with different concentrations exhibit strong adsorption at wavelengths of 220 and 277 nm. Through the increasing analyte concentration, the absorption increases in the mentioned wavelengths. From the obtained results it was found that the efficiency of extractions was in ordered as E_{II} (69 ± 1.80 %) > E_I (4.5 ± 0.35 %). It has seemed that among of many performed types of research to extract the natural products such as solid phase elements (SPE), Soxhlet, column chromatography and etc., the electrochemical extraction was shown the low-cost consuming, high speed and reasonable purity [22].

4. CONCLUSION

A thin film of Ppy/Pan/TiO_2/rGO was successfully coated on FTO glasses via the Electrophoretic-depositing techniques. Deposited film was characterized by FTIR, EIS, FESEM/EDX, and XRD. The conductivity of E_I and E_{II} were calculated from EIS results: 1.124 S/cm and 7.812 S/cm, respectively. From voltammetry method, it was found that the EgCg was an electroactive species and it was qualified (at -1 V) and the concentration of 10 ppm EgCg solution was quantified as 9.238, as well. Adsorption/desorption process was performed using E_I and E_{II} from standard and extracted solutions. The extracted EgCg was analyzed with HPLC and voltammetry techniques that those were shown comprised results. It was concluded that the extraction efficiency for mentioned adsorbents was E_{II} (76.02 ± 0.49%)>E_I (3.40 ± 0.05%).

ACKNOWLEDGEMENTS
We thank Advance Islamic Azad University of Gorgan branch providing valuable condition for research.

References

1. H. N. Graham, *Prev. Med.,* 21 *(*1992) 334.
2. Y. Hara, Green Tea: Health Benefits and Applications, Marcel Dekker, (2001), New York, America.
3. H. Wang, G. J. Provan, and K. Helliwell, *Trends Food Sci. Tech*., 11 (2000) 152.
4. J. H. Weisburger, E. Veliath, E. Larios, B. Pittman, E. Zang, and Y. Hara, *Mutat. R*es., 516 (2002) 19.
5. M. Suganuma, A. Saha and H. Fujiki, *Cancer Sci*., 102 (2011) 317.
6. M. Saltmarsh, C. Santos-Buelga and G. Williamson , Methods in Polyphenol Analysis, RSC (2003) Cambridge.
7. T. Yamamoto, L. R. Juneja, D-C. Chu and M. Kim, Chemistry and Applications of Green Tea*,* (1997) CRC Press, Boca Raton.
8. G. Rusak, D. Komes, S. Likić, D. Horžić and M. Kovač, *Food Chem.,* 110 (2008) 852.
9. D. Labbe, B. Tetu, D. Trudel, and L. Bazinet, *Food Chem*., 111 (2008) 139.
10. S. D. Sarker, Z. Latif and A. I. Gray, (Ed.), Natural Products Isolation*,* Humana Press (1998) Totowa.
11. M. Friedman, C. E. Levin, S.-H. Choi, E. Kozukue and N. Kozukue, *J. Food S*ci., 71 (2006) C328.
12. H. S. Park, H. J. Lee, M. H. Shin, K. W. Lee, H. Lee, Y. S. Kim, and K. H. Kim, *Food Chem*., 105

(2007) 1011.
13. T. J. Mason, L. Paniwnyk and J. P. Lorimer, *Ultrason. Sonochem*., 3 (1996) S253.
14. M. Tian, H. Yan, and K. H. Row, *Anal. Lett*., 43 (2010) 110.
15. X. Jun, J. Food Eng., 94 (2009) 105.
16. A. T. Bailey, D. Yuhasz and W. B. Zeng, US Patent, Hauser, Inc. United States, 09 (2001) 226477.
17. G. Yang, K. L. Kampstra and M. R. Abidian, *Adv. Mater*., 26 (2014) 4954.
18. U. Lange, N. V. Roznyatovskaya and V. M. Mirsky, *Analytica chimica acta*, 1 *(*2008) 1.
19. N. Puanglek, A. Sittattrakul and W. Lerdwijitjarud, Sci. J. UBU, 1 (2010) 35.
20. D. R. Dreyer, S. Park, C. W. Bielawski and R. S. Ruoff, *Chem. Soc. Rev*., 39 (2010) 228.
21. X. Tan, J. Wu, Q. Hu, X. Li, P. Li, H. Yu, X. Li and F. Lei, *Anal. Methods*, 7 (2015) 4786.
22. Q. V. Vuong, J. B. Golding, M. Nguyen, and P. D. Roach, *J. Sep. Sci.,* 33 (2010) 3415.
23. M. Ebadi, W. J. Basirun, Y. Alias, M. R. Mahmoudian and S. Y. Leng, *Mater. Charact.*, 66 (2012) 46.
24. A. Eftekhari, Nanostructured conductive polymers, Wiley (2010) Ohio USA.
25. P. Janeiro and A. M. O. Brett, Anal Chim Acta, 518 (2004) 109.
26. K. R. Markham, (Ed.), Techniques of flavonoid identification, Academic press, (1982), London UK.
27. C. Du, and N. Pan, *Nanotechnology*, 17 (2006) 5314.
28. M. Ebadi, M. Y. Sulaiman, M. A. Mat-Teridi, W. J. Basirun, M. A. Golsefidi, K. Sopian, A. Sateei, and R. Z. Mehrabian, *J. Appl. Electrochem*., 46 (2016) 645.
29. C. Huang, H. Bai, Y. Huang, S. Liu, S. Yen, and Y. Tseng, *Int. J. Photoenergy.,* 1 (2012) 1.
30. Y. Dong, Y. Zhou, Y. Ding, X. Chu and C. Wang, *Anal. Methods-Uk*, 6 (2014) 9367.
31. S. Xu, H. Yang, K. Wang, B. Wang and Q. Xu, *Phys. Chem*., 16 (2014) 7350.
32. J. Suárez-Guevara, O. Ayyad and P. Gómez-Romero, *Nanoscale Res. Lett*., 7 (2012) 521.
33. J. G. Wang, B. Wei and F. Kang, Rsc Adv, 4 (2014) 199.
34. G. K. Ramesha, A. V. Kumara, H. B. Muralidhara and S. Sampath, *J. Colloid Interface Sci*., 361 (2011) 270.
35. S. Masoum, M. Behpour, F. Azimi and M. H. Motaghedifard, *Sensor Actuat. B*, 193 (2014) 582.